International Journal of Minerals, Metallurgy and Materials
Volume 22, Number 7, July 2015, Page 661
DOI: 10.1007/s12613-015-1120-0

Effect of desliming on the magnetic separation of low-grade ferruginous manganese ore

Sunil Kumar Tripathy[1), *P.K. Banerjee*[1,2), *and Nikkam Suresh*[3)

1) Tata Steel Limited, Jamshedpur, Jharkhand, India
2) Hindalco Industries Limited, Aditya Birla Group, Mumbai, India
3) Indian School of Mines, Dhanbad, Jharkhand, India
(Received: 26 March 2015; revised: 17 April 2015; accepted: 20 April 2015)

Abstract: In the present investigation, magnetic separation studies using an induced roll magnetic separator were conducted to beneficiate low-grade ferruginous manganese ore. The feed ore was assayed to contain 22.4% Mn and 35.9% SiO_2, with a manganese-to-iron mass ratio (Mn:Fe ratio) of 1.6. This ore was characterized in detail using different techniques, including quantitative evaluation of minerals by scanning electron microscopy, which revealed that the ore is extremely siliceous in nature and that the associated gangue minerals are more or less evenly distributed in almost all of the size fractions in major proportion. Magnetic separation studies were conducted on both the as-received ore fines and the classified fines to enrich their manganese content and Mn:Fe ratio. The results indicated that the efficiency of separation for deslimed fines was better than that for the treated unclassified bulk sample. On the basis of these results, we proposed a process flow sheet for the beneficiation of low-grade manganese ore fines using a Floatex density separator as a pre-concentrator followed by two-stage magnetic separation. The overall recovery of manganese in the final product from the proposed flow sheet is 44.7% with an assay value of 45.8% and the Mn:Fe ratio of 3.1.

Keywords: manganese ore treatment; mineralogy; beneficiation; magnetic separation; flow sheet analysis

1. Introduction

Manganese is an important constituent of mild/carbon steel, stainless steel, and other alloys of manganese. The demand for manganese is increasing in parallel with the demand for steel, whereas high-grade manganese ores are being depleted. Thus, proper utilization of the available resources is a major challenge for the mining and minerals industry. However, the generation of large quantities of low-grade manganese ore as fines during mining and the size-grading of high-grade manganese ores have resulted in the accumulation of large amounts of inferior-quality ore that is being dumped at mine sites, resulting in space constraints and environmental problems [1−2]. Manganese ore deposits in India occur as bedded sedimentary deposits and are found predominantly in the states of Madhya Pradesh, Maharashtra, Gujarat, Andhra Pradesh, and Odisha. The Odisha state alone contributes 29% of the total Indian manganese ore reserves. These ores are ferruginous in composition and are inherently friable in nature [3]. The ore genesis of the Joda deposit is typical, where the gangue content is distributed in major proportion in all the size ranges [4−5]. The Joda mineral formation occupies a significant position in the geological map of India, in general, and in the manganese ores in particular. The mineralization of manganese ore in Odisha is mainly confined to three stratigraphic horizons, among which the ores of the iron-ore group occupy a larger area and mostly occur in the well-known horseshoe-shaped belt of banded iron formations of Precambrian age [3,6−7]. The manganese ores are mostly of low-to-medium-grade type with a low phosphorous content. In contrast to the other manganese deposits in Odisha, three varieties of low-grade manganese ores from this belt — (a) siliceous, (b) ferruginous and (c) aluminous types — have been reported [7−9]. Most of the manganese deposits of the Joda

Corresponding author: Sunil Kumar Tripathy E-mail: sunilk.tripathy@tatasteel.com

region are confined to pocket-type deposits, and their compositions differ from each other. These low-grade deposits, as well as the generated fines, can be utilized; however, a beneficiation process is imperative because of their high gangue content. Extensive research on beneficiation of different types of Indian manganese ores has been conducted [10−11], and some of the typical findings are discussed in the subsequent section.

2. Manganese ore beneficiation

The literature contains several technical reports and research papers related to the beneficiation of manganese ore. We here review and critically analyze some of the relevant published literature on this subject. Beneficiation flow sheets were developed for the reduction of alumina content in a lumpy manganese ore from the Joda area [12]. Simple classification and washing has been reported to result in sufficient reduction of the alumina and silica contents to 10%–14% with a recovery of 86%–88%. A floc-flotation study was conducted on ultrafine siliceous manganese ores from the Rida area of India [2], and the process parameters for improving the grade and recovery were optimized. Under the optimized conditions, the manganese ore was upgraded to 42.3% Mn at 38.2% recovery from a feed ore assayed to contain 27.8% Mn. Rao *et al.* [13] conducted magnetic separation studies on medium-grade manganese ores from the Chikla region of India and determined that the ores contained 44% Mn, 7.8% Fe, and 22% acid-insoluble components. When a wet high-intensity magnetic separator (WHIMS) was used, a concentrate assayed to contain 51% Mn was obtained with 95% recovery. Reduction roasting of manganese ore fines from the Tirodi region, India was performed using charcoal fines; this process was followed by magnetic separation to improve the fines' manganese-to-iron mass ratio (Mn:Fe ratio). Battery-grade manganese dioxide was produced by upgrading low-grade ores via chemical processing [14]. Similar studies were also conducted on Indian manganese deposits to improve the Mn:Fe ratio of the product through optimization of the reduction roasting process followed by magnetic separation [15−16]. However the techno-economics of these processes have yet to be addressed in the present scenario.

Low-grade siliceous manganese ores from the Bonai–Keonjhar belt, Orissa, India were mineralogically characterized and beneficiated by a combination of gravity and magnetic separation methods [17]. The results revealed that a feed having containing 26% Mn was upgraded to contain more than 45% Mn through the use of a dry-belt-type magnetic separator; 69% recovery was achieved at a magnetic field intensity of 1 T for finer-particle-size fractions. Low-grade manganese ores from the Gangpur Group of rocks (GG) were studied with respect to their field disposition, petrography, mineralogy, microstructure, and potential for being upgraded by physical methods [18]. The major manganese minerals were Mn-oxides (cryptomelane, pyrolusite, lithiophorite) with subordinate Mn-silicates in the bedded type, whereas manganese silicate phases (spessartite, braunite, rhodonite, etc.) dominated in the massive category. For the bedded-type ore, the product could be upgraded through a combination of dry and wet magnetic separation methods to 40.53% Mn with 24% yield from a feed assayed to contain 15% Mn.

The enrichment of the manganese content and the Mn:Fe ratio of a complex manganese ore from the Nishikhal deposit, India, containing 32% Mn, 18% Fe, 16% SiO_2, 21% acid-insoluble components, and 0.45% phosphorous was studied. By reduction roasting followed by magnetic separation, the Mn content of the product was enriched to 40% and the Mn:Fe ratio was increased to 10, although the phosphorous content decreased to 0.3% [19]. Beneficiation of low-grade manganese ore from Andhra Pradesh, India was investigated [20] using combination of jigging (for coarser sizes) and a WHIMS (for fines). The results of this study revealed that the product could be upgraded to 33% Mn from a feed assayed to contain 26.6% Mn, with an overall recovery of 50%. Another study on beneficiation of high-phosphorous, low-grade manganese ore from Andhra Pradesh, India using WHIMS was conducted; the results revealed that the manganese content of the sub-200-μm product could be upgraded in 6%–7% increments, with rejection of 10%–15% of insoluble gangue minerals. The authors also determined that the phosphorous content could not be reduced to less than 0.35% [21].

Recently, Singh *et al.* [11] briefly discussed the utilization and upgrading of low-grade manganese ore fines from the Joda region. The low-grade ore was screened at 0.5 mm, and the oversize product was treated in a circuit comprising gravity concentration and high-intensity magnetic separation. The authors adopted a gravity separation method (jigging and tabling) to remove the low-density silica and alumina mineral sand. Here, magnetic separation was required to improve the Mn:Fe ratio of the concentrate. In another study, a two-stage high-intensity magnetic separation process was established to recover a product assaying 42% Mn from a feed containing 32.4% Mn; the Mn:Fe ratio of the product was 5, and the manganese recovery was 47%–49% [22]. A permanent roll magnetic separator was used to separate braunite particles from metamorphic primary deposits from the Eskisehir region of Turkey, and the authors addressed the effect of particle size on particle separation [23]. Magnetic separation of the composite feed (−10+1 mm) particles was performed, and an approximate 10% enrichment in Mn was observed. The authors also concluded that pre-sizing of low-grade braunite ore into different particle size fractions did not significantly improve the separation efficiency in the magnetic separation compared to the separation efficiency achieved with the composite feed. This finding contradicts the basic theory of magnetic separation and is attributed to the improper liberation and intricate association of braunite-containing gangue in each of the size fractions. Further elucidation of the role of particle size in magnetic separation would require size-wise mineral analysis along with magnetic susceptibility distribution analysis.

Although alternative methods of beneficiation have been developed, the upgrading of manganese content is typically conducted by methods such as manual sorting (which is still practiced in some places), gravity concentration, flotation, and pre-concentration of manganese ore prior to the magnetic separation. As reported in the literature, the flotation of siliceous manganese ore has been attempted; however, the adsorption mechanism has not been properly addressed [2,24−26]. Gravity separation studies involving jigs, shaking tables, etc. have been used to upgrade siliceous manganese fines [27−29]. However, most of these studies have been limited to siliceous-type ore deposits. In general, the complexity of these separations is related to the liberation pattern of the manganese-bearing minerals and the gangue content. In some deposits, the alumina, silica, and iron gangue components are heterogeneous. Separation is believed to be easy when the ore contains gangue and manganese minerals with a large difference in their particle size, density, magnetic susceptibility, and hydrophobicity.

Most of the literature published on magnetic separation of manganese ores has been limited to siliceous-type ores (dominated by silicate-bearing gangue minerals), for which WHIMS has predominantly been used for upgrading at finer sizes. However, the literature contains very few studies on the dry magnetic separation of manganese from low-grade manganese ores with high silica and iron contents, except for a few attempts reduction roasting followed by magnetic separation. However, this process route cannot be commercialized because of its high operating costs in the present scenario. In this regard, a cost-effective techno-economic flow sheet has yet to be formulated for the utilization of these fines as a raw material in alloy making.

A thorough physical, chemical, and mineralogical characterization must precede the beneficiation of manganese ore fines. In most of the previously reported work, the low-grade ores were relatively rich in manganese and were studied for their beneficiation at coarser sizes. In the present work, manganese ore fines with very low manganese contents and with high silica and iron contents were used for the detailed characterization and subsequent magnetic separation studies. Furthermore, the effect of desliming on the separation of manganese-bearing particles under a magnetic field is highlighted and discussed. Also, a simplified flow sheet is suggested to beneficiate these ferruginous low-grade manganese ores.

3. Materials and methods

3.1. Manganese ore fines

Approximately 1 t of manganese fine was collected from the Joda opencast mine of Tata Steel at Odisha, India. The obtained sample was thoroughly mixed and sampled for characterization and experimental studies. Chemical analysis revealed that the collected ore fines were composed of 22.4% Mn, 14.5% Fe, 35.9% silica, and 3.8% alumina, giving an Mn:Fe ratio of 1.6. The characterization of the feed sample under study was performed using different techniques such as size analysis, size-wise chemical analysis, X-ray diffraction (XRD) analysis, mineralogical analysis (under an optical microscope), quantitative evaluation of minerals by scanning electron microscopy (QEMSCAN), and heavy-liquid analysis. The results are discussed in detail in the subsequent sections.

3.2. Experimental details

3.2.1. High-intensity dry magnetic separation

A high-intensity dry magnetic separator, known as an induced roll magnetic separator (IRMS), was used in the present investigation to concentrate the deslimed underflow material of the Floatex density separator as well as the as-received fines. Experiments were conducted at the laboratory scale using an IRMS supplied by Readings of Lismore, Australia. The magnetic intensity of the separator was varied by changing the gap and applied current (between the arc and rotor). In all of the tests, the magnetic intensity was varied by regulating the applied current and by maintaining the gap between the rotor and arc as constant at 3.2 mm. Similarly, the rotor speed was varied between 80 and 120 r/min while the feed rate was maintained at 0.25 t/h per meter width of rotor. Details related to the IRMS and the experimental procedure are well explained in the published literature [30]. Tests were conducted at different magnetic field intensities and rotor speeds. The products obtained from each of these tests were analyzed for estimation of the yield, grade, recovery, and enrichment of the Mn:Fe ratio.

3.2.2. Desliming studies

Desliming studies were conducted in a hydraulic, counter-current classifier to classify slime particles in the low-grade manganese ore. In the present study, statistically designed experiments were performed to beneficiate the siliceous manganese ore sample using a Floatex density separator (FDS, model LPF-0230, Outokumpu). The cross-sectional area of the square tank was limited to 0.23 m^2 and its height was 0.53 m. The elevation of the conical section was 0.2 m. The feed distributor was located 0.23 m from the top. The slurry was fed uniformly by controlling a bypass of the feed pipe connected to a separator and the agitator. A heavy-duty stirrer was fitted horizontally at the bottom level of the slurry tank to keep the slurry in uniform suspension. Before the start of an experiment, pre-determined quantities of manganese fines and water were mixed in the slurry tank to maintain a consistent feed at a uniform pulp density. The system was then allowed to run for a few minutes to attain a steady state. After ensuring the steady state condition through the slurry flow rates of the overflow and underflow streams, the products were collected for a known period and their respective weights were recorded for computing back-feed slurry rates for each of the experimental conditions. The collected slurry samples were weighed after being dried to determine their solids distribution and granulometry; the samples were also analyzed for grade, recovery, rejection, etc. A series of tests based on statistical design were conducted by varying the teeter water flow rate, set point, and other process variables such as the solids feed rate (0.5 t/h of dry solids) while the feed pulp density was kept constant at 25% solids by weight. The details of the variables studied and their levels maintained are presented in Table 1. Details about the FDS and the experimental procedure are well explained in the published literature [31].

Table 1. List of variables and their levels considered for the present study on FDS

No.	Process variables	Levels		
		Lower	Central	Higher
1	Teeter water flow rate / ($L\cdot min^{-1}$)	8	10	12
2	Set point	33	36	39
3	Feed rate / ($t\cdot h^{-1}$)		0.50	
4	Pulp density / wt%		25	

4. Results and discussion

4.1. Characterization studies

4.1.1. Size and size-wise chemical analyses

Wet-sieve analysis of manganese ore fines was conducted in the laboratory; the results of their population distribution are shown in Fig. 1. The results indicate that approximately 80% of the sample has a particle size less than 302 μm and that 33.6% of the total mass has a particle size less than 25 μm. The size-wise chemical analysis of the feed sample was performed to determine the distribution of manganese and its gangue content; the results are tabulated in Table 2.

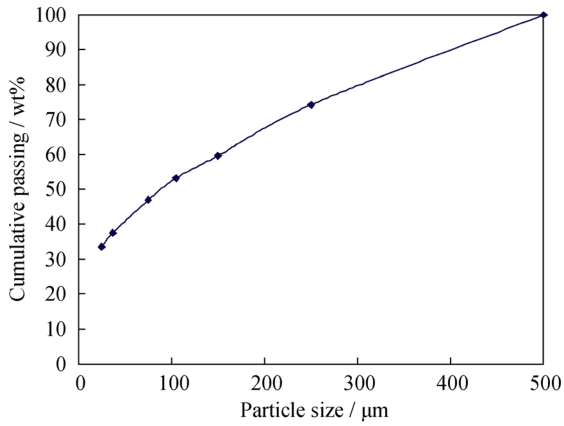

Fig. 1. Particle size distribution of manganese ore fines.

Table 2. Size-wise chemical analysis results of the manganese fines

Mesh size / μm	Weight retained / %	Assay value / wt%			
		Mn	$Fe_{(T)}$	SiO_2	Al_2O_3
+250	25.7	26.3	15.4	33.4	1.4
−250+150	14.8	19.6	13.1	48.0	1.2
−150+105	6.4	18.4	12.6	46.7	1.1
−105+75	6.3	19.1	13.3	45.0	1.3
−75+37	9.3	19.0	13.7	48.3	1.4
−37+25	4.0	17.8	12.9	49.2	1.3
−25	33.6	22.9	15.9	30.7	8.4

4.1.2. XRD studies

An XRD study was conducted to identify different mineral phases present in the ore; the obtained XRD patterns are shown in Fig. 2. These patterns indicate that pyrolusite, cryptomelane, and jacobsite are the manganese-bearing minerals, whereas quartz, hematite, and kaolinite are the major gangue minerals.

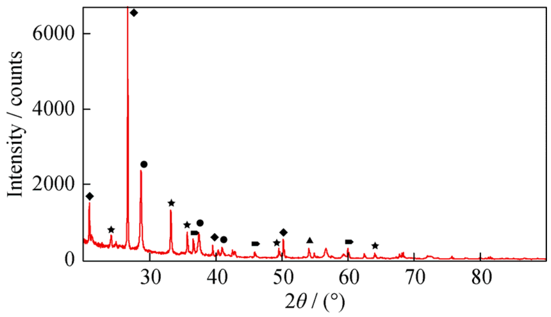

Fig. 2. XRD patterns of manganese ore fines with identified phases (◆Quartz, ★Hematite, ●Pyrolusite, ➨Cryptomelane, ✚Kaolinite, and ▲Jacobsite).

4.1.3. Mineralogical studies using an optical microscope

Mineralogical studies were conducted using an optical microscope to identify the different mineral phases present on the basis of the optical properties. The texture and the association of the manganese minerals with gangue were identified. The microphotographs of the ore are shown in Fig. 3. Most part of the manganese observed belongs to the mineral pyrolusite. Most of the silicate grains were interlocked with manganese minerals, as shown in Figs. 3(b) and 3(d). Large saccharoidal quartz grains were present along with manganese infillings. The observations also revealed that pyrolusite and cryptomelane constitute two distinct manganese phases (Fig. 3(d)). Pyrolusite occurs as large-bladed crystals having a sharp contact relationship with quartz (Fig. 3(b)), whereas thin veins of cryptomelane traverse through the sample. We also noted that cryptomelane and pyrolusite disseminated with silicate gangue minerals. The pyrolusite grains are present in the banded form along with quartz grains at different thickness (Fig. 3(c)).

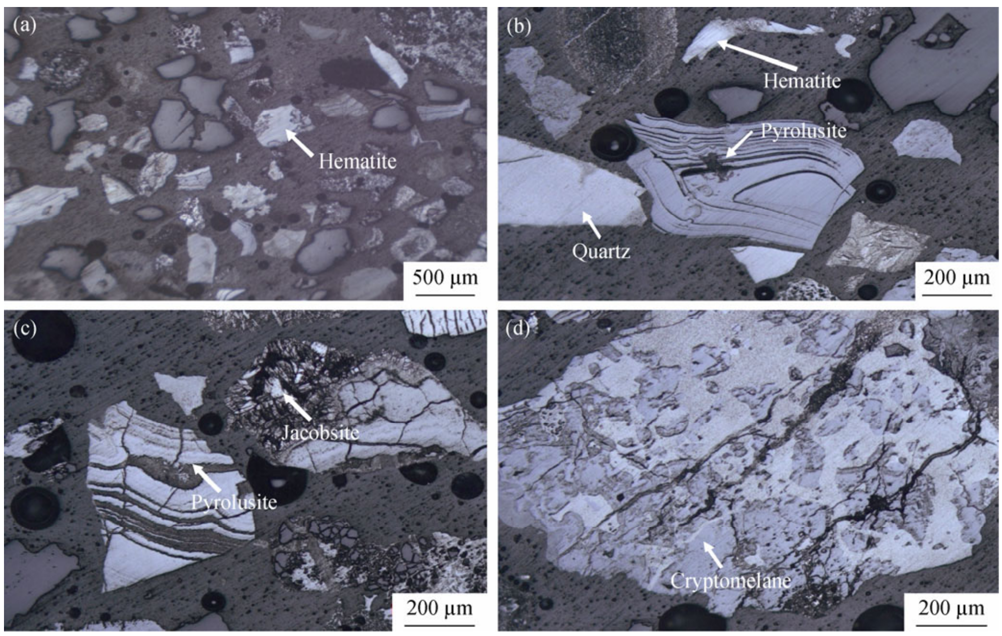

Fig. 3. Micrographs of manganese fines observed under an optical microscope.

4.1.4. Mineralogical analysis using QEMSCAN

To quantitatively estimate the mineral contents in the feed sample, we performed QEMSCAN, which gave quantitative modal mineralogical data related to trace mineral levels, the calculated chemistry, mineralogical association and liberation data, and elemental department with a mineralogical map of the sample. The mineral quantification of the feed sample was analyzed, as shown in Figs. 4(a)–4(b). As evident in Fig. 4(a), quartz, hematite, and kaolinite are the major gangue mineral phases, whereas pyrolusite, cryptomelane, braunite, and bixbyite are the manganese-bearing minerals in the ore. As also evident in the figure, 66% of the total feed contains manganese-bearing minerals, whereas quartz and hematite are the major gangue minerals (26%). Among the manganese-bearing minerals, pyrolusite is the dominant phase. The physical properties of the different minerals differ from each other, which provide an avenue for the beneficiation process. The deportment of Mn was subsequently derived and plotted in Fig. 4(b), which shows that approximately 50% Mn is from pyrolusite, whereas 26% is from braunite. The mineralogical map of the head sample is plotted in Fig. 5, which shows that most of the manganese-bearing minerals are in the free form, whereas the gangue minerals are in the interlocked form. Notably, the manganese-bearing minerals are in the liberated form at both coarser and finer sizes.

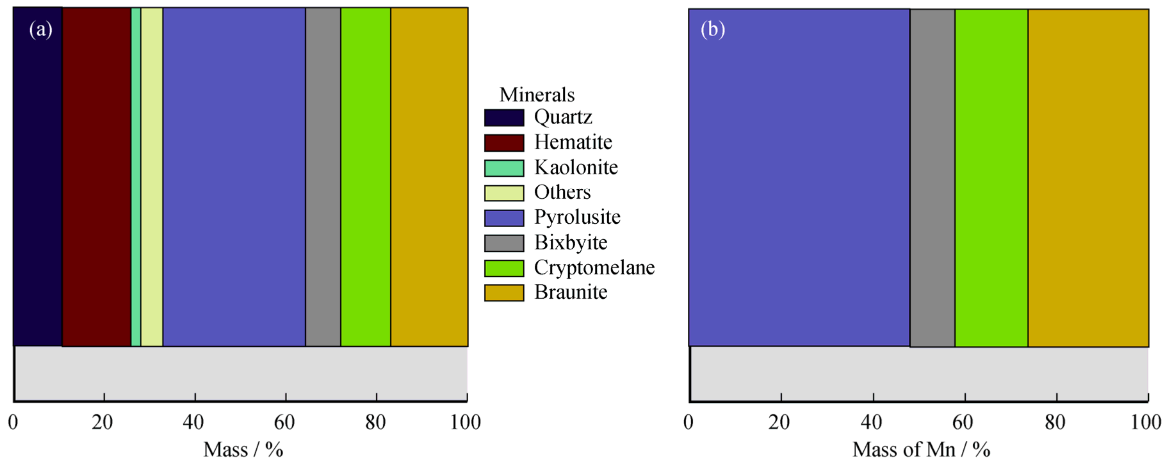

Fig. 4. Mineralogical studies in QEMSCAN: (a) quantification of different minerals in the ore fines; (b) deportment of manganese at different manganese minerals.

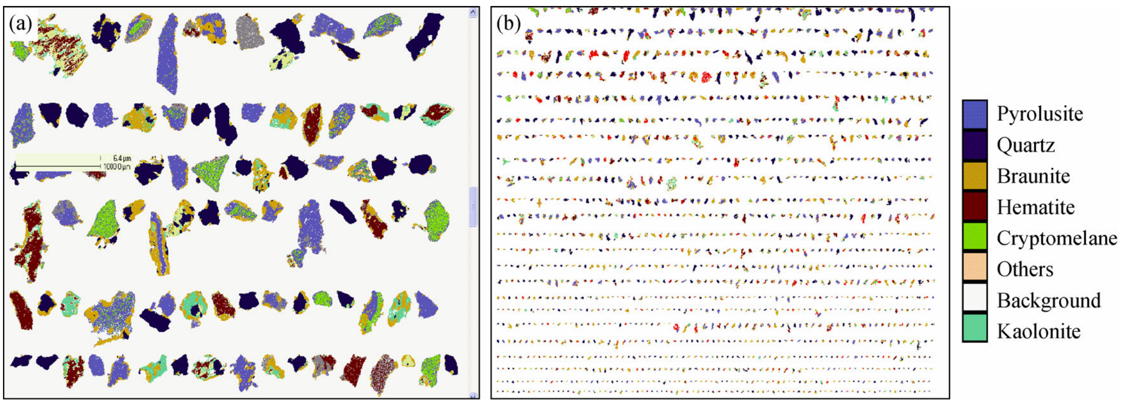

Fig. 5. Mineral mapping of head samples by using QEMSCAN: (a) coarser particle view; (b) finer particle view.

4.1.5. Heavy-liquid separation studies

Characterization by sink–float studies using heavy liquid was also performed to assess the quality of the sample. Pure bromoform (specific gravity 2.81) was used to quantify the heavy (specific gravity >2.81) and light (specific gravity <2.81) products of each size class of the manganese sample. The results indicated that the percentage of lower-specific-gravity material (gangue minerals) in the overall feed manganese sample is 21.2wt% (Table 3). In general, the proportion of light products tended to decrease with decreasing particle size. The high-weight percentage (50wt%) of the −105+75 μm material had a specific gravity less than 2.81. These results suggest that the float material is quartz, kaolinite, or other associated minerals.

Table 3. Results of sink and float study using bromoform

Size / μm	Weight / %	Float weight / %	Float weight (w.r.t. feed) / %
+250	25.7	31.8	8.2
−250+150	14.8	38.3	5.7
−150+105	6.4	43.0	2.8
−105+75	6.3	50.0	3.2
−75+37	9.3	9.7	0.9
−37+25	4.0	5.6	0.2
−25	33.6	1.0	0.3
Total	100		21.2

Note: w.r.t. means “with respect to”.

4.2. Magnetic separation studies

Magnetic separation tests were performed using an induced roll magnetic separator by varying the rotor speed and magnetic field intensity. The obtained results are given in Table 4. As evident from the results in the table, the manganese content could be enriched to a maximum of 27.5% at the higher rotor speed (120 r/min) and lower magnetic field intensity (0.8 T). The magnetic product obtained is not suitable for silicomanganese production because of its high gangue content in terms of iron and silica. In addition, the magnetic fraction separated by IRMS was enriched to

27.2% Mn and was obtained in higher yield than the previous fraction obtained at the higher rotor speed (120 r/min) and higher magnetic field intensity (1.6 T). Thus, the interactional effect of these two variables clearly plays a vital role in particle separation. However, in the products of the tests, the coating of the ultrafine particles (slime) on the coarse particle surface was observed to be predominant, which may be the reason for the poor separation of the manganese fines. Furthermore, the iron content of the non-magnetic products was low, but so was the manganese content. This result is a typical feature of this ore because it contains huge quantities of siliceous as well as iron-bearing gangue minerals. Evaluating the role of different variables on the efficiency of the separation was difficult. Thus, we formulated further strategies to classify the slime content prior to the magnetic separation.

Table 4. Magnetic separation of as-received manganese fines by varying the rotor speed and magnetic field intensity of IRMS

No.	Rotor speed / ($r \cdot min^{-1}$)	Magnetic field intensity / T	Products	Yield / %	Assay value / wt%			Mn:Fe ratio
					Mn	$Fe_{(T)}$	SiO_2	
1	80	0.8	Magnetic	74.2	24.5	16.2	31.7	1.5
			Non-magnetic	25.8	16.4	9.5	48.2	1.7
2	80	1.2	Magnetic	77.1	25.1	16.9	32.4	1.5
			Non-magnetic	22.9	13.4	6.2	47.9	2.1
3	80	1.6	Magnetic	83.7	24.3	16.1	33.8	1.5
			Non-magnetic	16.3	12.8	6.0	47.0	2.1
4	100	0.8	Magnetic	71.5	26.2	16.1	30.7	1.6
			Non-magnetic	28.5	12.9	10.3	49.1	1.3
5	100	1.2	Magnetic	75.6	27.1	16.7	30.9	1.6
			Non-magnetic	24.4	7.9	7.5	51.6	1.1
6	100	1.6	Magnetic	78.4	26.3	16.6	30.4	1.6
			Non-magnetic	21.6	8.3	6.7	56.1	1.2
7	120	0.8	Magnetic	58.2	27.5	17.1	28.9	1.6
			Non-magnetic	41.8	15.3	10.8	45.8	1.4
8	120	1.2	Magnetic	63.5	26.8	17.7	27.3	1.5
			Non-magnetic	36.5	14.8	8.8	51.0	1.7
9	120	1.6	Magnetic	67.2	27.2	17.2	26.9	1.6
			Non-magnetic	32.8	12.6	8.8	54.5	1.4

Note: Mn:Fe ratio means managnese-to-iron mass ratio.

According to the characterization results, gangue minerals such as iron- and silicate-bearing minerals are apparently evenly distributed in all of the size ranges. The silicate gangue minerals can be separated by gravity concentration because of their higher concentration criterion; however, these gangue minerals are distributed in all of the sizes in major proportion. Therefore, to suppress the particle size effect during separation, a pilot-scale Floatex density separator was used to reduce the content of siliceous gangue minerals. Because the Floatex density separator is an advanced hydraulic teeter bed separator, it separates particles on the basis of the principle of hindered settling coupled with fluidization. Meanwhile, for the removal of iron-bearing gangue minerals, magnetic separation was preferred, enabling exploitation of the magnetic susceptibility differences between different minerals. Therefore, the underflow product of FDS was treated in a high-intensity magnetic separator. The results of beneficiation studies are discussed further.

4.3. Classification studies using a Floatex density separator

Table 5 describes the experiments carried out with the Floatex density separator and presents the obtained results. With FDS, the manganese metal content was upgraded up to 42.1% from a feed Mn value of 22.4% in the underflow stream of FDS, with a simultaneous reduction in the silica content to 21.2% from 35.9% in the feed. The results also indicate that, as the teeter water flow rate increased, the yield to the underflow stream of FDS decreased. The yield value varied from 71.9% to 32.9%. In addition, as the set point increased, the bed height of the FDS also increased, resulting in higher yield values in the overflow stream.

Table 5. Underflow stream analysis results of FDS for all the tests

No.	Test conditions		Yield / %	Assay value / wt%	
	Teeter water flow rate/ $(L\cdot min^{-1})$	Set point		Mn	SiO_2
1	8	33	71.9	28.0	27.7
2	8	36	66.5	29.5	24.5
3	8	39	61.8	30.2	28.2
4	10	33	48.6	38.4	25.8
5	10	36	46.0	35.6	29.3
6	10	39	40.0	42.1	21.2
7	12	33	38.9	27.5	31.5
8	12	36	38.0	30.3	22.3
9	12	39	32.9	31.4	27.4

Results in Table 5 reveal that the Mn content in the underflow stream of the FDS was improved from 27.5% to 42.1%. The better product quality of the FDS underflow stream was achieved while the FDS was operated at intermediate teeter water flow rate, i.e., 10 L/min. At this flow rate, the Mn content varied from 35.6% to 42.1%; in contrast, at lower (8 L/min) and higher (12 L/min) teeter water flow rates, only a slight upgrade in Mn was observed in the underflow stream of FDS. This lack of upgrade is attributed to the fact that, with increasing teeter water flow rate, the teeter bed loosens and the density of the bed decreases. This decrease in density allows the lighter gangue minerals to also pass through the teeter bed to the underflow stream of the FDS. This particular phenomenon inside the teeter bed has been well described in the published literature [32]. In addition, the particle separation in the teeter bed also depends on the slip velocity. When the slip velocity of the particle is equal to the interstitial teeter water velocity, the particles will have a zero velocity with respect to a stationary observer and will have an equal probability to transport to either the overflow or the underflow stream. If the slip velocity is greater than the interstitial teeter water velocity, the particle will transport to the underflow stream; otherwise, it transports to the overflow stream [33–34]. That is, with the change (increase) in the set point, the quality of the underflow stream changes. Furthermore, the Mn content of the underflow stream significantly improves at higher set-point values because, at higher set-point values, the teeter bed height and bed pressure increase. Consequently, transport of the lighter gangue particles to the underflow is inhibited, thereby improving the quality of the underflow stream product.

The literature related to FDS reveals that it is an effective unit for removing silica gangue from iron ores, beach-sand minerals, chromite ores, etc. The present experimental results (Table 5) lead to a similar conclusion. Notably, the results of Table 5 indicate that, with change in teeter water flow rate and set point, the silica content in the underflow stream varied from 31.5% to 21.2%; however, an increase in the set point results in only a marginal decrease in the silica content . The recovery of Mn to the underflow stream and the rejection of silica to the overflow stream were analyzed; the results are presented in Fig. 6 for different teeter water conditions. As evident in Fig. 6, the recovery of the Mn content in the underflow stream varies from 89.7% to 46.1%. The recovery of Mn to the underflow stream decreased drastically at the higher teeter water flow rate (12 L/min, i.e., experiment Nos. 7, 8, and 9). Similarly the rejection of silica to the overflow stream increases with increasing teeter water flow rate. The maximum quantity of silica was rejected at the higher teeter water flow rate of 12 L/min. For better understanding of the factors that affect the recovery of Mn, we developed regression equations for Mn grade and recovery in the underflow stream of FDS. To correlate the effects of variables on the performance of FDS, the data presented in Table 5 were used to develop second-order quadratic equations using the mathematical software package MATLAB 7.1. The correlations thus developed are given by

$$\text{Manganese content in underflow (\%)} = -22.10 + 43.66\,TW - 9.38\,SP - 2.3\,TW^2 + 0.13\,SP^2 + 0.07\,TW \times SP \tag{1}$$

$$\text{Manganese recovery to underflow (\%)} = 79.27 + 30.65\,TW - 5.11\,SP - 2.38\,TW^2 + 0.03\,SP^2 + 0.2\,TW \times SP \tag{2}$$

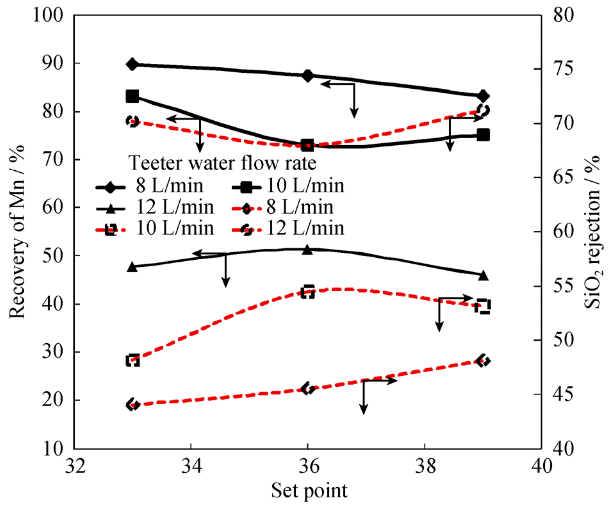

Fig. 6. Recovery of Mn to underflow and rejection of silica to overflow stream in all tests.

where TW is the teeter water flow rate, and SP is the set point. The Mn grade of the underflow product of FDS was computed using Eq. (1). The goodness of fit between the predicted values and the actual values for these correlations was evaluated by estimating the R^2 value (0.94). According to Eq. (1), the positive sign of the Mn grade of the underflow stream indicates that the Mn grade increases with increasing teeter water flow rate. The teeter water flow rate exerts greater influence on the grade of concentrate than does the set point. The interactional effect of the variables (teeter water flow rate and set point) on the grade of the underflow stream is negligible. The model equation for the Mn recovery of the underflow stream of FDS is given in Eq. (2), which again clarifies that the teeter water flow rate more strongly influences the Mn recovery in the underflow stream than does the set point or the mixed influence of teeter water flow rate and set point; however, a reverse effect is observed when the set-point value is increased.

Given the product grade and recovery of the underflow stream of FDS, the conditions in test No. 6 were chosen as the optimal conditions and were used to further improve the Mn:Fe ratio through removal of the iron-bearing gangue minerals. The target grade fixed for the optimization was such that the final product contained more than 40% Mn with maximum possible recovery. The partition values obtained under these conditions (for test No. 6) are shown in Fig. 7. When the cut size of the separation was 102 μm, the curve obtained resembled a typical Rosin–Rammler type (of particle size distribution) with a bypass ratio of 20%. The plot shows lower imperfections, implying that the misplacement of finer material into the underflow stream was low. Evidently, the set point and teeter water flow rate control the cut size and determine the performance of the FDS. A high set point and medium teeter water flow rate are most suitable for achieving a good separation in terms of manganese content in the underflow stream. However, high teeter water flow rates would be detrimental because it minimizes the rejection of manganese-bearing minerals to the overflow stream. These conditions provide efficient hydraulic transport, high misplacement, and a low residence time of the feed particles during concentration. These findings are contrary to the findings reported in the literature for the treatment of coal fines in FDS. For further improvement in the Mn content, the underflow stream product was treated by high-intensity magnetic separation; the results are further discussed in the next section.

4.4. Enrichment of FDS underflow product by high-intensity magnetic separation

The literature indicates that a high-intensity magnetic separator is an ideal unit for enhancing the Mn:Fe ratio in the low grade manganese ore [19–20,22]. The underflow stream product of FDS was treated in an IRMS by varying the magnetic field intensity and the rotor speed. The results of the tests are given in Table 6. At a lower rotor speed (80 r/min), the magnetic product was enriched with both manganese and iron-bearing minerals. Similarly, at greater magnetic field intensity, the non-magnetic product was enriched with silicate-bearing minerals. The effect of both of these operating parameters on the separation performance is discussed further.

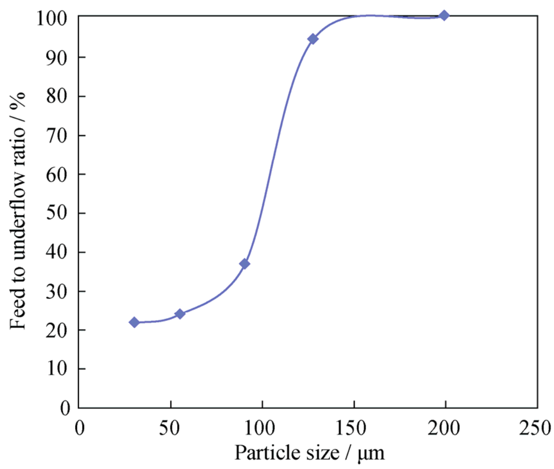

Fig. 7. Partition curve for Test No. 6.

In the magnetic separator, the applied magnetic field intensity was maintained by adjusting the input current. As the applied current increases, the magnetic field intensity will also be high at a given fixed gap between the rotor and the magnetic shoe. Another operating parameter, i.e., rotor speed, which imparts centrifugal force to the moving particle in the stream, is essentially a function of particle mass. However, because of the difference in the behavior of the classified feed constituents, i.e., manganese and iron-bearing minerals along with a limited amount of silicates, the mass of the iron-bearing minerals is identical to the mass of the manganese-bearing minerals. Also, the particle mass is an important parameter in this case because of the gravitational force. In these tests, the magnetic field intensity was varied from 0.8 to 1.6 T and the rotor speed was 80 or 100 r/min for treating the classified underflow stream product of FDS. The assay values of manganese in the magnetic products increased with increasing magnetic field intensity at a rotor speed of 100 r/min (Table 6) because of the unified susceptibility of the minerals. This result is due to the degree of selectivity as a function of the magnetic field intensity. Eventually, the optimum result was obtained at the lower rotor speed and a higher magnetic field intensity of 1.6 T, where the manganese content in the magnetic product was 44.5% with 86% Mn recovery. At lower magnetic field intensities, the locked particles (of manganese- and iron-bearing minerals) could not be picked-up by the rotor surface, which resulted in a relatively lower-grade product. Especially in the case of separation performed here, the manganese- and iron-bearing minerals were transported to the magnetic stream, whereas the silicate-bearing minerals were transported to the non-magnetic product. Under this optimized condition, the Mn:Fe ratio was observed to be very low, i.e., 2.2, because of the abundance of iron-bearing minerals, irrespective of their degree of liberation (free or locked). Because these magnetic particles exhibit a high magnetic susceptibility, they are picked up by the rotor surface. Similarly, the effect of the rotor speed being varied between 80 and 100 r/min was investigated, and the optimum result was achieved at the lower rotor speed of 80 r/min. The reason for this behavior could be that, in this type of magnetic separator, several forces act on the particles as they flow under the magnetic field, viz., centrifugal force, gravitational force, and magnetic force. In the present case, because the iron-bearing minerals and manganese-bearing minerals are distributed uniformly in all size fractions, differential centrifugal or gravitational forces cannot exist. This lack of differential forces is a consequence of the segregation of mono-size and mono-density particles of both minerals in the feed. Nevertheless, the difference in the magnetic susceptibility and the combined effect of these forces eventually determines the optimum operating conditions. As a result of this combination of forces, the optimum result, as represented by the manganese grade and recovery of magnetic product, was obtained at a magnetic field intensity of 1.6 T and a rotor speed at 80 r/min.

Table 6. Results of magnetic separation test for FDS underflow products

Test No.	Rotor speed / ($r \cdot min^{-1}$)	Magnetic intensity / T	Products	Yield / %	Assay value / wt%			Distribution value / %			Mn:Fe ratio
					Mn	$Fe_{(T)}$	SiO_2	Mn	$Fe_{(T)}$	SiO_2	
1	80	0.8	Magnetic	28.2	43.5	24.6	13.9	29.1	37.7	18.5	1.8
			Non-magnetic	71.8	41.3	16.0	25.6	70.4	62.4	86.9	2.6
2	80	1.0	Magnetic	32.1	43.2	23.6	14.6	32.9	41.2	22.2	1.8
			Non-magnetic	67.9	41.6	15.9	24.2	67.1	58.8	77.8	2.6
3	80	1.2	Magnetic	79.7	43.1	18.7	17.4	81.6	81.0	65.6	2.3
			Non-magnetic	20.3	38.2	17.2	35.9	18.4	19.0	34.5	2.2
4	80	1.4	Magnetic	80.8	43.8	19.5	16.3	84.0	85.6	62.3	2.2
			Non-magnetic	19.2	35.0	13.8	41.6	16.0	14.4	37.7	2.5
5	80	1.6	Magnetic	81.4	44.5	20.2	15.2	86.0	89.4	58.5	2.2
			Non-magnetic	18.6	31.6	10.5	47.2	14.0	10.6	41.5	3.0
6	100	0.8	Magnetic	24.1	42.9	23.8	14.4	24.6	31.2	16.4	1.8
			Non-magnetic	75.9	41.9	16.7	23.3	75.4	68.8	83.6	2.5
7	100	1.0	Magnetic	28.6	43.1	22.9	13.8	29.3	35.6	18.7	1.9
			Non-magnetic	71.4	41.7	16.6	24.1	70.7	64.4	81.3	2.5
8	100	1.2	Magnetic	65.7	43.5	18.7	16.2	67.9	66.8	50.3	2.3
			Non-magnetic	34.3	39.4	17.8	30.6	32.1	33.2	49.7	2.2
9	100	1.4	Magnetic	74.8	43.8	19.5	16.3	77.8	79.3	57.6	2.2
			Non-magnetic	25.2	37.1	15.1	35.5	22.2	20.7	42.4	2.5
10	100	1.6	Magnetic	76.4	44.1	20.3	15.8	80.0	84.3	57.1	2.2
			Non-magnetic	23.6	36.2	12.8	37.0	20.3	16.4	41.3	*2.8*
Feed					42.1	18.4	21.2				2.3

4.5. Flow-sheet development

Having established the optimum conditions for processing of ferruginous manganese ore from the Joda mine, we attempted to develop the process flowsheet because the Mn:Fe ratio in the beneficiated product was observed to be low, i.e., 2.2. This low Mn:Fe ratio necessitated that the ore be further re-treated. To increase the Mn:Fe ratio, a second stage of magnetic separation was used to effectively separate iron-bearing gangue minerals. Notably, the magnetic product of primary IRMS still contained some iron-bearing minerals that could not be separated. In this context, the magnetic fraction obtained from test No. 3 in Table 5 was further treated at a reduced magnetic intensity level of 0.8 T; the results of this test are shown in Table 7. As evident from the tabulated results, in the second stage of magnetic separation at lowered magnetic field intensity, the magnetic fraction was enriched with iron-bearing minerals, leaving much of the manganese in the non-magnetic stream and increasing the Mn:Fe ratio to 3.1.

Table 7. Results of second stage magnetic separation of manganese concentrate

Product	Yield / %	Assay value / wt%			Mn:Fe ratio
		Mn	$Fe_{(T)}$	SiO_2	
Magnetic	32.8	41.8	35.6	8.7	1.3
Non-magnetic	67.2	45.8	12.7	18.4	3.1
Feed		44.5	20.2	15.2	2.2

To summarize, in total, classification of Joda ferruginous ore using an FDS (Floatex density separator) discarded the maximum amount of silicate-bearing minerals; in contrast, further upgrading to achieve the desired Mn:Fe ratio was possible using two-stage magnetic separation. The detailed process flow diagram of the manganese ore fines is shown in Fig. 8. When FDS was used, approximately 75.1% of the Mn was recovered in its underflow stream, which had an acceptable grade of 42.1% Mn. In the first stage of magnetic separation by high-intensity IRMS at the higher magnetic field intensity of 1.6 T, the non-magnetic product was rich in silicate-bearing gangue material, whereas the magnetic product was enriched with manganese and a certain amount of iron-bearing minerals because of their paramagnetic properties. Further treatment of the ore at a lower magnetic field intensity of 0.8 T in the second stage resulted in the non-magnetic product being enriched with manganese and in a marginal amount of silicates by discarding most of the iron-bearing minerals in the magnetic stream. The final product of the process was enriched to 45.8% Mn with an Mn:Fe ratio of 3.1; in contrast, the manganese recovery was 44.7%. Similar studies were conducted by Grieco *et al.* [23] for the upgrading of braunite-rich particles by splitting the feed into several fractions and comparing the results with those obtained using bulk beneficiation. The results reported by Grieco *et al.* contradict the present findings. They observed that bulk separation was better split beneficiation. This difference in findings can be attributed to the distribution and abundance of the gangue-bearing slime coating on the coarse ore particles and also to the complex mineralogical association of the gangue.

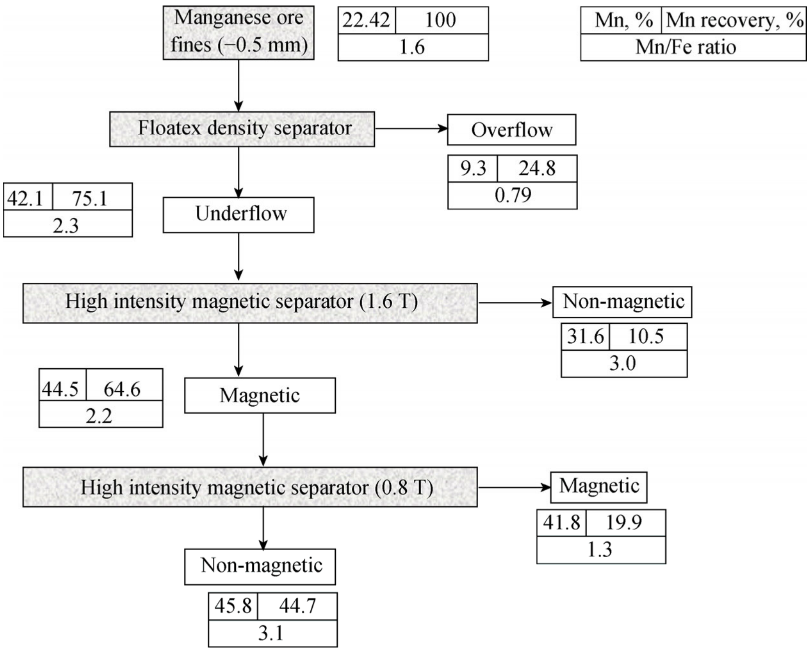

Fig. 8. Studied flow diagram for beneficiation of low grade manganese fines.

5. Conclusion

Low-grade manganese ore fines from the Joda region, India were studied in the present investigation; analysis of the ore fines indicated that they contained 22.4% Mn and 35.9% SiO_2, with an Mn:Fe ratio of 1.6. Detailed characterization studies by size and chemical analysis, XRD analysis, mineralogical analysis, and optical microscopy in combination with QEMSCAN and heavy-liquid studies were conducted prior to magnetic separation. The following points were concluded: (1) approximately, 21wt% of the total mass was low-density gangue minerals, which can easily be separated by initially differentiating the particles by size and density; (2) in the ore, 50wt% of the manganese minerals were in the liberated form, whereas the remainder was intricately associated with the gangue minerals in different proportions.

On the basis of the results of the characterization, beneficiation of low-grade manganese fines was conducted by subjecting both the as-received sample as well as classified mass to magnetic separation. We drew the following conclusions. (1) Magnetic separation of as-received samples indicated poor separation of manganese-bearing minerals because of the abundance of slime content in the feed. (2) These fines were classified using a Floatex density separator to deslime the feed; the Floatex density separator classified the feed and rejected the maximum amount of silicate-bearing gangue minerals in the overflow, whereas the two-stage magnetic separation of its underflow gave an appreciable upgrade of the Mn content, along with an acceptable Mn:Fe ratio. (3) Beneficiation studies of low-grade manganese ore fines using a Floatex density separator resulted in an increase in the manganese content to 42.1% Mn with 75.1% recovery; in contrast, two-stage magnetic separation facilitated in discarding of the silicates and iron-bearing gangue minerals. (4) In two-stage magnetic separations, i.e., high-magnetic field intensity followed by low-magnetic field intensity, of the FDS deslimed product, an enriched Mn:Fe ratio of 3.1 was achieved through separation of the silicates and iron-bearing gangue minerals. (5) On the basis of our findings, we proposed a process flow sheet for the beneficiation of low-grade manganese ore fines. The overall recovery of manganese in the final product was 44.7%, with an assay value of 45.8% and an Mn:Fe ratio of 3.1. This suggested simplified flow sheet will improve the recovery substantially for the production of silico/ferromanganese-grade concentrate from the fines. The additional recovery of manganese may require that the middling product be reground and retreated with multiple passes through a high-intensity induced roll magnetic separator.

References

[1] K.S. Mani and D. Subrahmanyam, Utilisation of low grade/off grade ores and mine waste, *Proc. Indian Natn. Sci. Acad.*, 50A(1984), p. 509.

[2] P.K. Naik, P.S.R. Reddy, and V.N. Misra, Floc flotation studies of ultra fine siliceous manganese ore by linear orthogonal saturated design, *J. Min. Metall.*, 41A(2005), p. 11.

[3] S. Roy, Ancient manganese deposits, [in] K.H. Wolf, *Handbook of Strata-Bound and Stratiform Ore Deposits*, Elsevier Scientific Publishing Company, Amsterdam, 1976, p. 395.

[4] B.C. Acharya, D.S. Rao, and R.K. Sahoo, Nishikhal manganese deposit, Koraput District, Orissa, *J. Geo. Soc. India*, 36(1990), No. 6, p. 644.

[5] B.C. Acharya, D.S. Rao, and R.K. Sahoo, Mineralogy and genesis of Kutinga manganese deposit, South Orissa, India, *J. Mineral. Petrol. Econ. Geol.*, 89(1994), No. 8, p. 317.

[6] S. Roy, Classification of manganese deposits, *Acta Mineral. Petrol.*, 19(1969), p. 67.

[7] P. Mishra, B.K. Mvohapatra, and P.P. Singh, Mode of occurrence and characteristics of Mn-ore bodies in iron ore group of rocks, North Orissa, India and its significance in resource evaluation, *Res. Geol.*, 56(2006), No. 1, p. 55.

[8] B.K. Mohapatra, S. Mishra, and P.P. Singh, Biogenic wad in Iron Ore Group of rocks of Bonai–Keonjhar belt, Orissa, *J. Geol Soc. India*, 80(2012), No. 1, p. 89.

[9] K.V.G.K. Gokhale and T.C. Rao, *Ore Deposits of India*, Affiliated East West Press, New Delhi, 1983.

[10] P.I.A. Narayan and N.N. Subrhmanyan, *Beneficiation of Low Grade Manganese Ores of India*, CSIR, New Delhi, 1957.

[11] V. Singh, S.M. Rao, T.K. Ghosh, C.R. Kumar, and T.C. Rao, Beneficiation of low grade manganese ore fines to recover ferromanganese grade concentrate, *Tata Search*, 2009, No. 1, p. 155.

[12] V. Singh, S.M. Rao, A. Dixit, and B.K. Das, Developing process flow sheet for reducing the alumina content in lumpy manganese ore feed for ferromanganese plant, *Tata Search*, 2006, No. 1, p. 47.

[13] G.V. Rao, B.K. Mohapatra, and A.K. Tripathy, Enrichment of the manganese content by wet high intensity magnetic separation from Chikla manganese ore, India, *Magn. Electr. Sep.*, 9(1998), No. 2, p. 69.

[14] T. Sharma, Physico-chemical processing of low grade manganese ore, *Int. J. Miner. Process.*, 35(1992), No. 3-4, p. 191.

[15] Y.V. Swamy, B. Bhoi, S. Prakash, and H.S. Ray, Enrichment of the manganese to iron ratio of ferruginous low-grade manganese ore using solid reductant, *Miner. Metall. Process.*, 15(1998), p. 34.

[16] V. Kivinen, H. Krogerus, and J. Daavittila, Upgradation of Mn:Fe ratio of low grade manganese ore for ferromanganese production, [in] *Proceedings of XII International Ferro Alloys Congress*. Helsinki, 2010, p. 467.

[17] P.P. Mishra, B.K. Mohapatra, and K. Mahanta, Upgradation of low-grade siliceous manganese ore from Bonai–Keonjhar belt, Orissa, India, *J. Miner. Mater. Charact. Eng.*, 8(2009), No. 1, p. 47.

[18] N. Dash, B.K. Mohapatra, and D.S. Rao, Petro-minerographical studies of off-grade Mn-ores from two contrasting occurrences in Gangpur Group of rocks, India, and their influence on beneficiation, *World Metall. Erzmetall*, 63(2010),

No. 2, p. 5.

[19] G.V. Rao, B.C. Acharya, B.V.R. Murty, J.N. Mohanty, Y.V. Swamy, P. Chattopadhay, and A.K. Tripathy, Removal of phosphorus and enrichment of manganese from a complex ferruginous manganese ore, *Magn. Electr. Sep.*, 9(1998), No. 2, p. 109.

[20] S.B. Kanungo, S.K. Mishra, and D. Biswal, Beneficiation of low-grade, high phosphorous manganese ores of Andhra Pradesh, India, by wet high-intensity magnetic separation plus jigging or hydrocyclone classification, *Miner. Metall. Process*., 17(2000), No. 4, p. 269.

[21] S.B. Kanungo, S.K. Mishra, and D. Biswal, Beneficiation of low grade, high phosphorous manganese ores of Andhra Pradesh, India, by wet high intensity magnetic separation, *Miner. Metall. Process*., 17(2000), No. 3, p. 181.

[22] V. Singh, T.K. Ghosh, Y. Ramamurthy, and V. Tathavadkar, Beneficiation and agglomeration process to utilize low-grade ferruginous manganese ore fines, *Int. J. Miner. Process*., 99(2011), No. 1-4, p. 84.

[23] G. Grieco, S. Kastrati, and M. Pedrotti, Magnetic enrichment of braunite-rich manganese ore at different grain sizes, *Miner. Process. Extr. Metall. Rev.*, 35(2014), No.4, p.257.

[24] T.V. Dendyuk, New reagent systems for flotation of low-grade manganese products of combined beneficiation, *Powder Technol*., 71(1992), No. 1, p. 47.

[25] M. Oliazadeh, M. Noaparast, and R. Dehghan, Beneficiation of low grade fine manganese ores, [in] *Proceeding of the XXIII International Mineral Processing Congress*, Istanbul, 2006, p. 347.

[26] A.M. Abeidu, The feasibility of activation of manganese minerals flotation, *Trans. JIM*, 14(1973), p. 45.

[27] E.L. Chanturiya, T.V. Bashlykova, N.I. Potkonen, and A.R. Makavetskas, Poor manganese ore dressing on the basis of mineralogical–technological studies, [in] *Proceedings of the XXI International Mineral Processing Congress*, Rome, 13(2000), p. C2-1.

[28] M.R. Hosseini, A. Bahrami, and M. Pazouki, Influence of shaking table parameters on manganese grade and recovery, [in] *Proceedings of the XXIV International Mineral Processing Congress* (*IMPC*), Beijing, 2008, p. 783.

[29] U. Malayoglu, Study on the gravity processing of manganese ores, *Asia J. Chem*., 22(2010), No. 4, p. 3292.

[30] S.K. Tripathy, P.K. Banerjee, and N. Suresh, Separation analysis of dry high intensity induced roll magnetic separator for concentration of hematite fines, *Powder Technol.*, 264(2014), p. 527.

[31] S.K. Tripathy, M.K. Mallick, V. Singh, and Y.R. Murthy, Preliminary studies on teeter bed separator for separation of manganese fines, *Powder Technol*., 239(2013), p. 284.

[32] S. Roy, S.K. Mandal, and A. Das, Segregation and process features in a teeter bed separator as revealed by high-speed videography and image processing, *Miner. Process. Extr. Metall. Rev*., 35(2014), No.1, p.15.

[33] B. Sarkar, A. Das, S. Roy, and S.K. Rai, In depth analysis of alumina removal from iron ore fines using teetered bed gravity separator, *Miner. Process. Extr. Metall.*, 117(2008), No. 1, p. 1.

[34] C.R. Kumar, S. Mohanan, S.K. Tripathy, Y. Ramamurthy, T. Venugopalan, and N. Suresh, Prediction of process input interactions of Floatex Density Separator performance for separating medium density particles, *Int. J. Miner. Process*., 100(2011), No. 3-4, p. 136.